Niğde Ömer Halisdemir Üniversitesi Mühendislik Bilimleri Dergisi
Nigde Omer Halisdemir University Journal of Engineering Sciences

ISSN: 2564-6605
Araştırma / Research

ANALYSIS OF DYNAMIC BEHAVIOR OF PERMANENT MAGNET SYNCHRONOUS MOTORS AND CONTROLLING CHAOS WITH NONLINEAR OUTPUT REGULATION

Handan NAK[1], Ali Fuat ERGENÇ[2,*]

[1,2] *Control and Automation Engineering Department, Istanbul Technical University*

ABSTRACT

In this paper, the dynamic behavior of permanent magnet synchronous motors and the nonlinear output regulation of them for constant reference signals are studied. The dynamic analysis is based on previous studies and new results related to chaos phenomena are obtained. With the state feedback control law, regulation of motor velocity and direct-axis current is achieved for known and unknown load torque at constant operating points. Moreover, the control law is enhanced in the sense of robustness with respect to parameter uncertainties by utilizing an augmented system with integral operators.

Keywords: Chaos, PMSM, Nonlinear output regulation problem, Feedback control, Robustness.

SABİT MIKNATISLI SENKRON MOTORUN DİNAMİK DAVRANIŞ ANALİZİ VE DOĞRUSAL OLMAYAN KONTROLÖR İLE KAOS KONTROLÜ

ÖZET

Bu çalışmada sabit mıknatıslı senkron motorların dinamik davranışları analiz edilmiş ve sabit referans sinyali için doğrusal olmayan çıkış regülasyon kontrolü işlenmiştir. Dinamik analiz literatürde var olan çalışmalara dayandırılarak kaos olayına ilişkin yeni sonuçlar elde edilmiştir. Belirli ve belirsiz yük momentleri altında sabit çalışma noktasında motor hız regülasyonu ve direkt eksen akımı durum geri beslemesi kontrolü ile sağlanmıştır. Bunun ötesinde kontrol kuralı integral içeren yardımcı sistem vasıtasıyla parametre belirsizliklerine karşı dayanıklılık anlamında geliştirilmiştir.

Anahtar kelimeler: Kaos, SMSM, Doğrusal olmayan regülasyon problemi, Geri beslemeli Kontrol, Dayanıklılık

1. INTRODUCTION

In recent years, permanent magnet synchronous motors (PMSM) with their numerous advantages are extensively utilized in every field of industry including automation, automotive, space, computer, medical electronics, military applications, robotics and small household applications. Advancements in material science and electronics relieve manufacturing costs and enhances the properties of permanent magnets which deliver highly efficient motors with smooth and constant torque, high torque/current and torque/inertia ratio. Obviously, in many critical applications stable and safe operation of PMSM is an indispensable request. However, Hemati pointed out in his studies [1] and [2] that PMSM with certain system parameter values and under some operating conditions generates chaotic behaviors which may even destroy the system stability, and more detailed studies on PMSM chaos phenomenon were done in [3] and [4]. Thus, not surprisingly there are various studies focused on controlling and overcoming chaos in PMSM [5-15].

Dong et al. [5] studied a state feedback control law that renders PMSM system passive on the basis of study [16]. Ren and Liu presented a nonlinear feedback controller method to suppress chaos and stabilize the system about a set-point without the proof of stability [6]. Moreover, Ren et al. [7] successfully implemented the method of time delay feedback control of PMSM. Wei et al. revealed that the dynamic time delay feedback method can stabilize the states over a much larger domain of parameters compared to the static delay time feedback [8]. In another study, Wei et al. proposed an adaptive dynamic surface control of chaos in PMSM [9]. On the other hand, Loria presented a solution for set-point and tracking with parameter uncertainties output regulation problem with showing uniform global asymptotic stability of PMSM using cascaded theory [10]. The studies [11] and [12] are examples of Lyapunov exponents methods to control PMSM.

* Sorumlu yazar / Corresponding author, e-posta / e-mail: ali.ergenc@itu.edu.tr
Geliş / Recieved: 08.10.2019 Kabul / Accepted: 12.12.2019 doi: 10.28948/ngumuh.630680

Essentially, the purpose of control problem of the PMSM is to design a feedback control law that stabilizes the closed-loop system, and lets motor speed asymptotically track a reference signal and regulates direct-axis current to a set point (mostly zero) under the presence of the load torque. Therefore, this problem can be considered as output regulation problem for a nonlinear system as defined by Isidori and Brynes in [17]. Based on this idea Huang and Ping studied the control problem of PMSM with internal model design employing the general framework established in [18]. In [14], authors studied output regulation problem of surface-mounted PMSM with any reference input generated by some exosystem and uncertain motor parameters with known bounds. They expanded the work by studying general case of PMSM (non-smooth air gap PMSM) in [15]. However, their approach generates nonlinear control laws, and needs definite bounds for exact constant load torque and perturbations of motor parameters.

In this paper, first we present some new results related to the stability properties of PMSM. In the literature, there are two different affine linear transformations for dq reference frame PMSM equations, [1] and [3]. In [3], Li et al. proposed a transformation which converts physical parameters of the motor into two constants σ and γ. Because of physical constraints, σ is always a positive constant while γ is negative. However, they assigned a positive value to γ that changes stability analysis entirely. Furthermore, many studies in the literature [3, 4, 6, 9-13, 19-21] are based on the ground of this analysis. In our study, we prove that PMSM never demonstrates chaotic phenomena when the external inputs are removed. We also present that even if motor parameters are not in bifurcation region, PMSM may generate chaotic behaviors depending on the initial conditions of the states.

The larger part of the study contains solving the output regulation problem of nonlinear PMSM system with linear state feedback control law when reference inputs and disturbances (load torque) are constant signals. We use directly the method that proposed by Isidori and Brynes for this purpose [17]. First, it is presented that the regulation of all three states of PMSM is not possible by using state feedback. Therefore, we solve the regulation problem of only two states (motor speed and direct-axis current) which is sufficient and acceptable for PMSM control system. Afterwards, the robustness of the system is improved against measurement noise and parametric time varying uncertainties utilizing the integrator action, and then the output regulation problem for that "augmented" plant is solved. The proposed control law is linear and easy to implement. The law does not require any information about load torque except that it has constant derivative w.r.t time. Furthermore, the bounds for parametric uncertainty that maintain the closed loop stability are determined by controller matrix K. Finally, the theoretical findings are validated through simulation studies.

The rest of the paper is organized as follows. In Section 2, the transformed mathematical model of PMSM is reviewed. In Section 3, new results for chaos and bifurcation analysis of PMSM are presented. In Section 4 the principles of nonlinear output regulation problem are given. In Section 5, the solution for nonlinear output regulation problem of PMSM with state feedback regulator for set-point control is exhibited and discussed. Then, the robustness properties are improved. In Section 6, several simulation results are presented, and finally the study is concluded in Section 7.

2. MACHINE MODEL

The dynamic equations of PMSM in dq reference frame is written as [22]

$$\frac{di_d}{dt} = \frac{1}{L_d}(-R\, i_d + n_p\, \omega L_q i_q + v_d) \tag{1a}$$

$$\frac{di_q}{dt} = \frac{1}{L_q}(-R\, i_q - n_p\, \omega L_d i_d - \omega\varphi_r + v_q) \tag{1b}$$

$$\frac{dw}{dt} = \frac{1}{J}(\frac{3}{2} n_p \varphi_r i_q + \frac{3}{2} n_p (L_d - L_q)\, i_q i_d - T_L - b\, \omega) \tag{1c}$$

where i_q and i_d are quadrature-axis and direct-axis currents, v_q and v_d are quadrature-axis and direct-axis voltages, L_q and L_d are quadrature-axis and direct-axis stator inductances, R is winding resistance; n_p is number of permanent pole pairs, φ_r is permanent-magnet flux constant, b is viscous friction coefficient, T_L is load torque, J is moment of inertia, and ω is angular rotor velocity. Note that for a smooth-air-gap PMSM $L_q = L_d = L$ in the model (2).

In literature PMSM equations in (1) are transformed into another environment via an affine linear transformation and time scaling to provide convenience for analysis, control and design [1-3, 10, 23]. They consider an affine linear transformation of the form

$$\mathbf{x} = \Sigma\, \tilde{\mathbf{x}} + \zeta \tag{2}$$

where $\mathbf{x} = [\omega\ \ i_q\ \ i_d]^T$; Σ is a 3×3 constant nonsingular diagonal matrix, and ζ is a 3×1 constant vector. They also consider a time-scaling of the form

$$t = \tau \tilde{t} \tag{3}$$

to obtain a nondimeonsionalized form. In this context, two different transformations with the same output equation set come into prominence. One of them is introduced by Hemati [2], and Σ, ζ, and τ are defined as follows for smooth-air-gap PMSM:

$$\tau = \frac{L_q}{R} \tag{4}$$

$$\Sigma = \begin{bmatrix} \sigma_1 & 0 & 0 \\ 0 & \sigma_2 & 0 \\ 0 & 0 & \sigma_3 \end{bmatrix} = \begin{bmatrix} \frac{R}{n_p L} & 0 & 0 \\ 0 & \frac{2b}{3 n_p^2 \tau \varphi_r} & 0 \\ 0 & 0 & \frac{2b}{3 n_p^2 \tau \varphi_r} \end{bmatrix} \tag{5}$$

$$\zeta = \begin{bmatrix} \zeta_1 \\ \zeta_2 \\ \zeta_3 \end{bmatrix} = \begin{bmatrix} 0 \\ 0 \\ \frac{-(2/3 \rho L b + n_p^2 \varphi_r^2 \tau)}{n_p^2 \varphi_r L \tau} \end{bmatrix} \tag{6}$$

then, the system in (1) can be written in the form

$$\dot{\tilde{x}}_1 = \sigma (\tilde{x}_2 - \tilde{x}_1) - \tilde{T}_L \tag{7a}$$
$$\dot{\tilde{x}}_2 = -\tilde{x}_2 - \tilde{x}_1 \tilde{x}_3 + \rho \tilde{x}_1 + \tilde{v}_q \tag{7b}$$
$$\dot{\tilde{x}}_3 = -\tilde{x}_3 + \tilde{x}_1 \tilde{x}_2 + \tilde{v}_d \tag{7c}$$

where ρ is a free parameter, and $\sigma = \frac{\tau b}{J}, \tilde{T}_L = \frac{n_p \tau^2}{J} T_L, \tilde{v}_q = \frac{3 n_p^2 \tau^2 \varphi_r}{2 L b} v_q,$ and $\tilde{v}_d = \frac{3 n_p^2 \tau^2 \varphi_r}{2 L b} v_d + \frac{2 \rho L b + 3 n_p^2 \varphi_r^2 \tau}{2 L b}$.

On the other hand, the other most cited transformation is studied by Li *et al.* in [3]. They set ζ equal to zero, and define Σ and τ as follows:

$$\tau = \frac{L_q}{R} \tag{8}$$

$$\Sigma = \begin{bmatrix} \sigma_1 & 0 & 0 \\ 0 & \sigma_2 & 0 \\ 0 & 0 & \sigma_3 \end{bmatrix} = \begin{bmatrix} \frac{1}{\tau} & 0 & 0 \\ 0 & k & 0 \\ 0 & 0 & \delta k \end{bmatrix} \tag{9}$$

where $k = \frac{2b}{3 n_p^2 \tau \varphi_r}$ and $\delta = \frac{L_d}{L_q}$. Then the following equation system is obtained:

$$\dot{\tilde{x}}_1 = \sigma (\tilde{x}_2 - \tilde{x}_1) + \varepsilon \tilde{x}_2 \tilde{x}_3 - \tilde{T}_L \tag{10a}$$
$$\dot{\tilde{x}}_2 = -\tilde{x}_2 - \tilde{x}_1 \tilde{x}_3 + \gamma \tilde{x}_1 + \tilde{v}_q \tag{10b}$$
$$\dot{\tilde{x}}_3 = -\delta \tilde{x}_3 + \tilde{x}_1 \tilde{x}_2 + \tilde{v}_d \tag{10c}$$

where $\gamma = -\frac{\varphi_r}{k L_q}, \sigma = \frac{\tau b}{J}, \tilde{v}_q = \frac{1}{R k} v_q, \tilde{v}_d = \frac{1}{R k} v_d, \varepsilon = \frac{\delta \tau k (L_d - L_q)}{J \varphi_r}$ and $\tilde{T}_L = \frac{n_p \tau^2}{J} T_L$.

In the transformation developed by Hemati, in the case of $L_q \neq L_d$, the same equation set with (10) is obtained with different Σ and ζ matrices, and again with a free parameter ρ; for more details, see [1].
For simplicity only smooth-air-gap PMSM is studied ($L_q = L_d = L$), and the dynamic model in (10) becomes

$$\dot{\tilde{x}}_1 = \sigma (\tilde{x}_2 - \tilde{x}_1) - \tilde{T}_L \tag{11a}$$
$$\dot{\tilde{x}}_2 = -\tilde{x}_2 - \tilde{x}_1 \tilde{x}_3 + \gamma \tilde{x}_1 + \tilde{v}_q \tag{11b}$$
$$\dot{\tilde{x}}_3 = -\tilde{x}_3 + \tilde{x}_1 \tilde{x}_2 + \tilde{v}_d. \tag{11c}$$

Note that, since difference of the definition of electromagnetic torque, there is a minor coefficient change in the transformations. Also, note that the equation sets (7) and (11) have the same structure except one important point; ρ and γ parameters. In (7), ρ is a free parameter, while in (11) γ is a negative valued parameter whose value depends on motor characteristics.

3. NEW RESULTS IN CHAOS AND BIFURCATION ANALYSIS

At first, we consider the case of which, the external inputs are set to zero, namely, $v_d = 0$, $v_q = 0$, and $T_L = 0$ after an operation of the system.

This case corresponds to $\tilde{v}_d = 0$, $\tilde{v}_q = 0$, and $\tilde{T}_L = 0$ in (2); and the transformed system becomes identical to the Lorenz equation. The equilibrium points of the dynamic system are $(0{,}0{,}0)$ and $(\pm\sqrt{\gamma-1}, \pm\sqrt{\gamma-1}, \gamma-1)$. It is seen that the origin is an equilibrium for any values of the parameters. The other two equilibria are real if and only if $\gamma \geq 1$. However, it is not possible since γ only depends on the motor parameters and it is always less than zero as mentioned before. To investigate the stability of origin we use Lyapunov's theorem; consider the function

$$V(x) = \frac{1}{2}(-\gamma\,\tilde{x}_1^{\,2} + \sigma\,\tilde{x}_2^{\,2} + \sigma\,\tilde{x}_3^{\,2}). \tag{12}$$

The parameter constraints $\gamma < 0$ and $\sigma > 0$ ensure that over the domain R^3, $V(x)$ is continuously differentiable, $V(0) = 0$ and $V(x) > 0$ for all $x \neq 0$. Then,

$$\dot{V}(x) = \gamma\,\tilde{x}_1^{\,2} - \sigma\,\tilde{x}_2^{\,2} - \sigma\,\tilde{x}_3^{\,2} \leq 0. \tag{13}$$

Therefore, $\tilde{x} = 0$ is stable. Moreover, $\dot{V}(x) \leq 0$ in $R^3 - \{0\}$, so $\tilde{x} = 0$ is asymptotically stable. This $\tilde{x} = 0$ point is equal to $(w, i_q, i_d) = (0{,}0{,}0)$ in original dq motor equations.

That result can be verified by also using Hemati's transformation in [2]. If the external inputs are removed ($v_d = v_q = T_L = 0$), then $\tilde{v}_d = \frac{2\,\rho\,L\,b + 3\,n_p\,\varphi_r{}^2\,\tau}{2\,L\,b}$, $\tilde{v}_q = 0$, and $\tilde{T}_L = 0$. Equilibrium points become $(0{,}0, \tilde{v}_d)$ and $(\pm\sqrt{\rho - 1 - \tilde{v}_d}, \pm\sqrt{\rho - 1 - \tilde{v}_d}, \rho - 1)$. The two nontrivial equilibria makes sense only when $\rho - \tilde{v}_d > 1$. However, it is not possible regardless of the value of ρ. Again by using Lyapunov's theorem one can show that the first equilibrium point $(0{,}0, \tilde{v}_d)$ is asymptotically stable; and this equilibria is equal to the origin in original dq motor equations.

As a consequence, after a period of operation, if the external inputs of the system are removed, there is only one equilibrium point, which is $(w, i_q, i_d) = (0{,}0{,}0)$. This point is always asymptotically stable and PMSM never demonstrates chaotic behavior in that case on the contrary what is studied in a large number of articles [3, 6, 9, 11, 13, 19].

In studies [4, 6, 9-13, 19-21], authors used transformation of Li *et al.* in [3] which is given in (10) and (11), however in their analysis and simulations they gave a positive value to γ parameter. Correspondingly, they could find chaotic behavior of PMSM in case of removed inputs.

Another investigated case is $v_d \neq 0$, $v_q = 0$, and $T_L = 0$. In this case we utilize the transformation in [2] due to its simplicity; we can still say $\tilde{v}_q = 0$ by just adjusting the value of ρ (it is a free parameter in the transformation). Here, the equation set in (7) is identical to Lorenz equation.

It is possible to prove that the solutions of the Lorenz equations are bounded. There exists a bounded region E such that every trajectory eventually enters E and never thereafter leaves it [24]. When $\rho \leq 1$ origin is the only equilibrium point and all solutions are attracted to the origin as we showed before. When $\rho > 1$, three real equilibrium points occur; $(0{,}0{,}0)$ and $(\pm\sqrt{\rho-1}, \pm\sqrt{\rho-1}, \rho-1)$. Let us call these three points as $C0$, $C1$, and $C2$ respectively. To determine the stability of these points, the Jacobian matrix of the system (7) is checked as follows

$$J(\tilde{x}_1, \tilde{x}_2, \tilde{x}_3) = \begin{bmatrix} -\sigma & \sigma & 0 \\ -\tilde{x}_3 + \rho & -1 & -\tilde{x}_1 \\ \tilde{x}_2 & \tilde{x}_1 & -1 \end{bmatrix}. \tag{14}$$

For the point $C0$, the Jacobian matrix $J(0{,}0{,}0)$ is block diagonal. The eigenvalues are $-1, \frac{-1-\sigma\pm\sqrt{1-2\,\sigma+4\,\rho\,\sigma+\sigma^2}}{2}$. Note that for $\rho \leq 1$, all there eigenvalues are negative. For $\rho > 1$, the Jacobian matrix has one positive real and two negative real eigenvalues. Hence, the stable node at the origin becomes an unstable manifold.

For the points $C1$ and $C2$, eigenvalues of Jacobian matrix are roots of the polynomial

$$p(\lambda) = \lambda^3 + (2+\sigma)\,\lambda^2 + (\sigma+\rho)\lambda + 2\,\rho\,\sigma - 2\,\sigma. \tag{15}$$

Note that stability characteristics of $C1$ and $C2$ are the same because of their symmetry. For ρ near 1, roots of $p(\lambda)$ are negative real. There is a point ρ_{ns} that causes a change in the character of the equilibria $C1$ and $C2$ from nodes to spirals. For $\sigma > 2$ and $\rho_{ns} < \rho < \rho_h = \frac{\sigma(\sigma+4)}{\sigma-2}$, one of the eigenvalues is negative real, other two are complex conjugate and have negative real parts. Therefore, $\rho = \rho_h$ is a Hopf bifurcation point of the system and $C1$ and $C2$ are stable equilibrium points for $\rho < \rho_h$ [3]. For $\rho > \rho_h$ real parts of all eigenvalues are positive and PMSM losses its stability.

However, it is not possible to claim that if $\rho < \rho_h$, the equilibrium points $C1$ and $C2$ are asymptotically stable. The most characteristic feature of a chaotic system is its unpredictability. The solutions of differential equations strongly depend on initial conditions. Small changes in an initial state can make a very large difference in the behavior of the system.

We illustrate this phenomenon by an example. Let the system parameters be $\sigma = 5$ and $\rho = 14$ ($\rho_h = 15$). Then the equilibrium points are $C0 = (0,0,0)$, $C1 = (-3.605, -3.605, 13)$, $C2 = (3.605, 3.605, 13)$, and eigenvalues of Jacobian matrix are $\lambda_0 = (-11.602, 5.602, -1)$, $\lambda_{1,2} = (-6.955, -0.022 + 4.323\,i, -0.022 - 4.323\,i)$. For different initial conditions, different behavior of PMSM is seen in Fig. 1, Fig. 2 and Fig. 3. Hence, for $\rho < \rho_h$ it can only be said that the solutions are bounded. For general case of v_d, v_q and T_L, one can see [3] and [4].

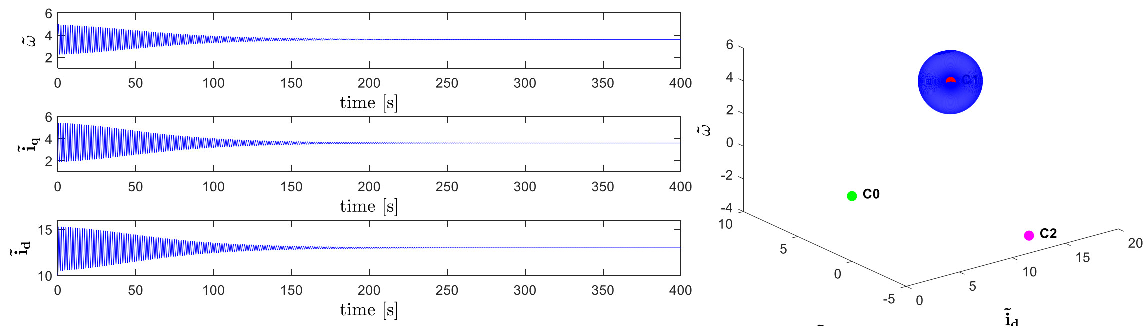

Figure 1. For initial condition $\tilde{\omega}(0) = 5, \tilde{\imath}_q(0) = 2, \tilde{\imath}_d(0) = 10$ results for time simulation and generated stable node.

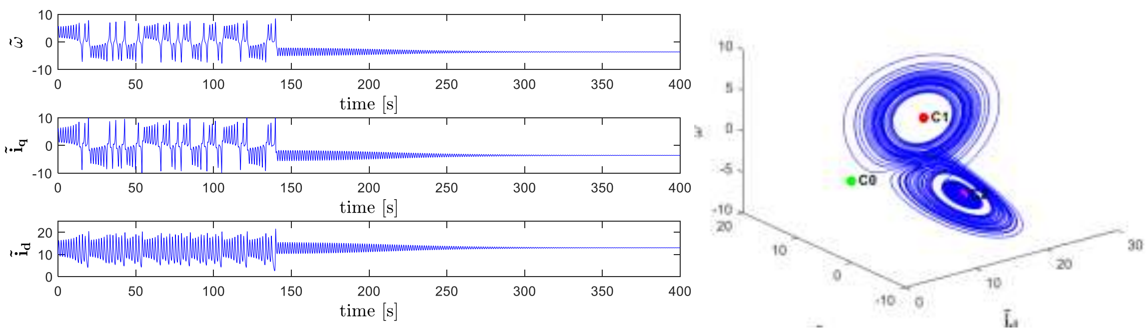

Figure 2. For initial condition $\tilde{\omega}(0) = 5, \tilde{\imath}_q(0) = 5, \tilde{\imath}_d(0) = 10$ results for time simulation and generated pre-chaotic attractor.

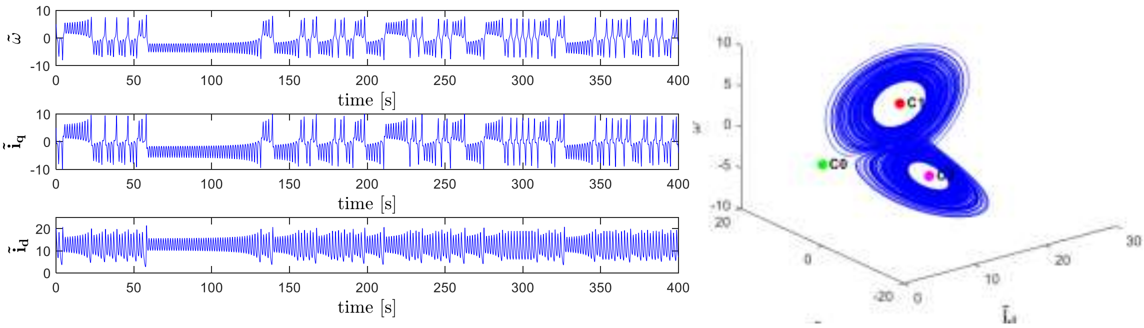

Figure 3. For initial condition $\tilde{\omega}(0) = 5, \tilde{\imath}_q(0) = 5, \tilde{\imath}_d(0) = 20$ results for time simulation and generated chaotic attractor.

Therefore, it is important to design a control law satisfying two requirements. The first one is guaranteeing the asymptotic stability of the closed loop system, the second one is asymptotic tracking of reference inputs in the presence of disturbances. In this paper, our aim is to control the chaos in PMSM using output regulation theory for nonlinear systems.

4. OUTPUT REGULATION PROBLEM FORMULATION

Consider a multivariable nonlinear plant described by

$$\dot{x} = f(x) + g(x)u + p(x)w \tag{16}$$

$$\dot{w} = s(w) \tag{17}$$

$$e = h(x) + q(w) \tag{18}$$

where x is the plant state defined on a neighborhood X of the origin $\mathbf{R}^n$, $u \in \mathbf{R}^m$ is the control input, w, defined on neighborhood W of the origin $\mathbf{R}^s$, is an *exogenous* signal which includes references to be tracked and disturbances, and $e \in \mathbf{R}^p$ is the regulated output. The first equation describes the dynamics of the plant, while the second equation describes *exosystem*, and models disturbances and reference signals taken into consideration. The regulated output in the third equation is mostly chosen as tracking error between the actual output $h(x)$ and reference signal $q(w)$.

The vectorfields/functions $f(x)$, $g(x)$, $p(x)$, $s(w)$, $h(x)$, and $q(w)$ are assumed to be continuously differentiable mappings. It is also assumed that $f(0) = 0$, $s(0) = 0$, $h(0) = 0$, $q(0) = 0$. Thus, for $u = 0$, the system (16) and (17) has an equilibrium state $(x, w) = (0,0)$ with zero error (18).

In [17], Isidori and Brynes defined *state feedback regulator problem* as follows:

Problem: Find, if possible, $u = \alpha(x, w)$ such that [a)]

1. the equilibrium point $x = 0$ of

$$\dot{x} = f(x) + g(x)\alpha(x, 0) \tag{19}$$

is exponentially stable;

2. there exists a neighborhood $U \subset X \times W$ of (0,0) such that, for each initial condition $(x(0), w(0)) \in U$, the solution of (16) satisfies

$$\lim_{t\to\infty} h(x(t)) + q(w(t)) = 0. \tag{20}$$

They solved the problem under following assumptions [17]:

H1: $w = 0$ is a stable equilibrium of the exosystem, and there exists a neighborhood $\widehat{W} \subset W$ of the origin with the property that initial condition $w(0) \in \widehat{W}$ is Poisson stable.

H2: The pair $f(x)$, $g(x)$ has a stabilizable linear approximation at $x = 0$.

Theorem 1: Under the hypotheses H1 and H2, the state feedback regulator problem is solvable if, and only if, there exist C1 mappings $x = \pi(w)$ with $\pi(0) = 0$ and $u = c(w)$, with $c(0) = 0$, both defined in a neighborhood of $W^0 \subset W$ of 0, satisfying the conditions

$$\frac{\delta\pi}{\delta w} s(w) = f(\pi(w)) + g(\pi(w))c(w) + p(\pi(w))w \tag{21}$$

$$h(\pi(w)) + q(w) = 0 \tag{22}$$

When the Byrnes-Isidori regulator equations (21) and (22) are satisfied, a control law solving the state feedback regulator problem is given by

$$\alpha(x,w) = c(w) + K[x - \pi(w)] \tag{23}$$

where K is any gain matrix that makes linear approximation of the system stable [17].

5. OUTPUT REGULATION PROBLEM OF PMSM

Generally in PMSM drive systems, the control objective motor velocity, ω, is desired to be constant. Since, ω is relative to the quadrature-axis current, i_q, the desired value of i_q is calculated according to ω. The direct-axis current, i_d, can be set any constant value depending on control strategy, such as it is set to zero in field oriented control. Therefore, the reference signals of all states are constant (set-point control). Also, the motor load T_L is assumed to be a constant disturbance signal in the study. Naturally, in the control scheme, the voltages v_q and v_d are controlled input variables.

5.1 Regulation of all State Variables

In this section, it is desired that all states to track constant reference signals. Consider the overall PMSM plant with reference and disturbance signals described by

$$\dot{\tilde{x}}_1 = \sigma\,(\tilde{x}_2 - \tilde{x}_1) - w_1 \tag{24a}$$
$$\dot{\tilde{x}}_2 = -\tilde{x}_2 - \tilde{x}_1\,\tilde{x}_3 + \gamma\,\tilde{x}_1 + \tilde{v}_q \tag{24b}$$
$$\dot{\tilde{x}}_3 = -\tilde{x}_3 + \tilde{x}_1\,\tilde{x}_2 + \tilde{v}_d \tag{24c}$$
$$e_1 = \tilde{x}_1 - w_2 \tag{24d}$$
$$e_2 = \tilde{x}_2 - w_3 \tag{24e}$$
$$e_3 = \tilde{x}_3 - w_4. \tag{24f}$$

where w_1 denotes motor load $\tilde{T}_L$, and w_2, w_3, w_4 are denote reference signals for $\tilde{x}_1$, $\tilde{x}_2$ and $\tilde{x}_3$ respectively. Note that the inputs of the system are $u = [v_q \;\; v_d]^T$.

The exosystem is defined as $w = [w_1 \;\; w_2 \;\; w_3 \;\; w_4]^T$, and given by the scalar dynamics

$$\dot{w} = 0. \tag{25}$$

It is important to observe that the exosystem is neutrally stable because the solutions of (38) are only constant trajectories [25]. Thus, assumption H1 of Theorem 1 holds trivially.

Linearizing the dynamics of the system in (24) at the origin, we get the system matrices

$$A = \left[\frac{d\,f(x)}{d\,x}\right]_{x=0} = \begin{bmatrix} -\sigma & \sigma & 0 \\ \gamma & -1 & 0 \\ 0 & 0 & -1 \end{bmatrix} \tag{26a}$$

$$B = \left[\frac{d\,g(x)}{d\,x}\right]_{x=0} = \begin{bmatrix} 0 & 0 \\ 1 & 0 \\ 0 & 1 \end{bmatrix}. \tag{26b}$$

Kalman's rank test for controllability, reveals that the pair (A, B) is completely controllable except the case $\sigma = 0$ which is not possible because of psychical system ($\sigma > 0$, see section 2). Thus, the assumption H2 of Theorem 1 also holds. Hence, Theorem 1 can be applied to solve the output regulation problem for the system (24).

The regulator equations of (24) are obtained as

$$0 = \sigma(\pi_2(w) - \pi_1(w)) - w_1 \tag{27a}$$
$$0 = -\pi_2(w) - \pi_1(w)\,\pi_3(w) + \gamma\,\pi_1(w) + c_1(w) \tag{27b}$$
$$0 = -\pi_3(w) + \pi_1(w)\,\pi_2(w) + c_2(w) \tag{27c}$$
$$0 = \pi_1(w) - w_2 \tag{27d}$$
$$0 = \pi_2(w) - w_3 \tag{27e}$$
$$0 = \pi_3(w) - w_4. \tag{27f}$$

The equations in (27) are solvable only when $w_3 = \frac{w_1}{\sigma} + w_2$. Hence, by Theorem 1, we conclude that the output regulation problem is not solvable for this case if $w_3 \neq \frac{w_1}{\sigma} + w_2$. However, it is not reasonable to fulfill this condition because it limits the reference choices. Also, it requires the knowledge of load torque, T_L (w_1).

As mentioned before the main control objective is motor velocity. The value of i_q current changes to provide desired motor velocity, and i_d current reference is independent from these two variables. Therefore, it is sufficient to regulate the motor velocity and i_d current to control the PMSM.

5.2 Regulation of Two State Variables

In this case, it is desired to regulate ω and i_d, namely $\tilde{x}_1$ and $\tilde{x}_3$ states respectively. Consider the plant

$$\dot{\tilde{x}}_1 = \sigma\,(\tilde{x}_2 - \tilde{x}_1) - w_1 \tag{28a}$$
$$\dot{\tilde{x}}_2 = -\tilde{x}_2 - \tilde{x}_1\,\tilde{x}_3 + \gamma\,\tilde{x}_1 + \tilde{v}_q \tag{28b}$$
$$\dot{\tilde{x}}_3 = -\tilde{x}_3 + \tilde{x}_1\,\tilde{x}_2 + \tilde{v}_d \tag{28c}$$
$$e_1 = \tilde{x}_1 - w_2 \tag{28d}$$
$$e_2 = \tilde{x}_3 - w_3. \tag{28e}$$

where w_1 denotes motor load $\tilde{T}_L$, w_2 and w_3 are denote reference signals for $\tilde{x}_1$ and $\tilde{x}_3$ respectively. This time, the exosystem is defined as $w = [w_1\;\; w_2\;\; w_3]^T$. The dynamics of exosystem and linearized system matrices (A, B) are same with the previous case in (25) and (26). Thus assumptions H1 and H2 of Theorem 1 hold. Hence, Theorem 1 can be applied to the system (5.2).

The regulator equations of (28) are obtained as

$$0 = \sigma(\pi_2(w) - \pi_1(w)) - w_1 \tag{29a}$$
$$0 = -\pi_2(w) - \pi_1(w)\,\pi_3(w) + \gamma\,\pi_1(w) + c_1(w) \tag{29b}$$
$$0 = -\pi_3(w) + \pi_1(w)\,\pi_2(w) + c_2(w) \tag{29c}$$
$$0 = \pi_1(w) - w_2 \tag{29d}$$
$$0 = \pi_3(w) - w_3. \tag{29e}$$

Solving the regulator equations in (29), we have the solution

$$\pi_1(w) = w_2 \tag{30a}$$
$$\pi_2(w) = \frac{w_1}{\sigma} + w_2 \tag{30b}$$
$$\pi_3(w) = w_3 \tag{30c}$$
$$c_1(w) = \frac{w_1}{\sigma} + w_2 + w_2\,w_3 - \gamma\,w_2 \tag{30d}$$
$$c_2(w) = -\frac{w_1\,w_2}{\sigma} - {w_2}^2 + w_3. \tag{30e}$$

By Theorem 1, a state feedback control law solving the output regulation problem is given by (23). Here, K is a 2×3 matrix, and control law is formed as

$$\tilde{v}_q = c_1(w) + k_{11}(\tilde{x}_1 - \pi_1(w)) + k_{12}(\tilde{x}_2 - \pi_2(w)) + k_{13}(\tilde{x}_3 - \pi_3(w)) \tag{31a}$$
$$\tilde{v}_d = c_2(w) + k_{21}(\tilde{x}_1 - \pi_1(w)) + k_{22}(\tilde{x}_2 - \pi_2(w)) + k_{23}(\tilde{x}_3 - \pi_3(w)). \tag{31b}$$

Assume that load torque T_L (consequently, w_1) is known. Then, finding a gain matrix K such that $A + B\,K$ in (5.1) is Hurwitz, solves the state feedback regulator problem of the system (28).

Let us assume now that load torque is unknown. In this case, we can eliminate the load torque knowledge from control law in (31) by tuning the gains in K matrix such that $k_{12}=1$ and $k_{22}=-w_2$. At this stage, it may seem that the internal stability of the controller depends on reference signal for velocity (w_2), and this is not acceptable. Nevertheless, a little analysis reveals that the eigenvalues of $A+BK$ are independent from w_2 if $k_{13}=0$. This approach is not irrational since $\tilde{v}_q$ voltage is not required to contain information about $\tilde{\iota}_d$ current. Then (31) becomes

$$\tilde{v}_q = w_2\, w_3 - w_2\, \gamma + k_{11}(\tilde{x}_1 - w_2) + \tilde{x}_2 \tag{32a}$$

$$\tilde{v}_d = w_3 + k_{21}(\tilde{x}_1 - w_2) - w_2\, \tilde{x}_2 + k_{23}(\tilde{x}_3 - w_3). \tag{32b}$$

As seen from (32), the knowledge of load torque is not required in this case. Other gains (k_{11}, k_{21}, k_{23}) are determined to achieve internal stability of state feedback regulator problem.

5.3 Augmented System for Robustness

It may be reasonable argued that the control law (5.2) may present poor performance under parametric variations since it has a constant part that depends on motor parameter γ. Even if the motor parameters are known precisely, once motor starts to turn, winding temperature rises and stator winding resistance and inductances will change. Therefore, some precautions must be taken.

For this purpose, we present an integral control approach. The use of integral control ensures the output regulation under parameter perturbations that do not destroy the stability of closed-loop system. Parameter perturbations force equilibrium point to change, but through the instrument of integral action, desired equilibrium point will be maintained. Thus, as long as the perturbed equilibrium point remains asymptotically stable, regulation will be achieved [26]. To apply integral action, we integrate the regulation errors and add them to the control signal. Then, the following “augmented” plant with 2 additional states ξ_1 and ξ_2 is obtained.

$$\dot{\tilde{x}}_1 = \sigma\,(\tilde{x}_2 - \tilde{x}_1) - w_1 \tag{33a}$$

$$\dot{\tilde{x}}_2 = -\tilde{x}_2 - \tilde{x}_1\,\tilde{x}_3 + \gamma\,\tilde{x}_1 + \xi_1 + \tilde{v}_q \tag{33b}$$

$$\dot{\tilde{x}}_3 = -\tilde{x}_3 + \tilde{x}_1\,\tilde{x}_2 + \xi_2 + \tilde{v}_d \tag{33c}$$

$$\dot{\xi}_1 = w_2 - \tilde{x}_1 \tag{33d}$$

$$\dot{\xi}_2 = w_3 - \tilde{x}_3 \tag{33e}$$

$$e_1 = \tilde{x}_1 - w_2 \tag{33f}$$

$$e_2 = \tilde{x}_3 - w_3. \tag{33g}$$

The control task now is to find a control law ($\tilde{v}_q$, $\tilde{v}_d$) pair that solves the output regulation problem of the augmented plant. Finally, augmented control law will become,

$$\tilde{v}_{qa} = \xi_1 + \tilde{v}_q \tag{34a}$$

$$\tilde{v}_{da} = \xi_2 + \tilde{v}_d. \tag{34b}$$

The exosystem is identical with the previous case. Thus assumption H1 of Theorem 1 holds. Linearizing the augmented plant at $x=0$, we obtain

$$A_a = \left[\frac{d\, f_a(x_a)}{d\, x_a}\right]_{x_a=0} = \begin{bmatrix} -\sigma & \sigma & 0 & 0 & 0 \\ \gamma & -1 & 0 & 1 & 0 \\ 0 & 0 & -1 & 0 & 1 \\ -1 & 0 & 0 & 0 & 0 \\ 0 & 0 & -1 & 0 & 0 \end{bmatrix} \tag{35a}$$

$$B_a = \left[\frac{d\, g_a(x_a)}{d\, x_a}\right]_{x_a=0} = \begin{bmatrix} 0 & 0 \\ 1 & 0 \\ 0 & 1 \\ 0 & 0 \\ 0 & 0 \end{bmatrix}. \tag{35b}$$

The pair (A_a, B_a) is completely controllable except the case $\sigma=0$ which is not reasonable as mentioned before. Thus assumption H2 of Theorem 1 also holds. Therefore, Theorem 1 can be applied to the system (33).
The regulator equations of (33) are obtained as

$$0 = \sigma(\pi_2(w) - \pi_1(w)) - w_1 \tag{36a}$$
$$0 = -\pi_2(w) - \pi_1(w)\,\pi_3(w) + \gamma\,\pi_1(w) + \pi_4(w) + c_1(w) \tag{36b}$$
$$0 = -\pi_3(w) + \pi_1(w)\,\pi_2(w) + \pi_5(w) + c_2(w) \tag{36c}$$
$$0 = w_2 - \pi_1(w) \tag{36d}$$
$$0 = w_3 - \pi_1(w) \tag{36e}$$
$$0 = \pi_1(w) - w_2 \tag{36f}$$
$$0 = \pi_3(w) - w_3. \tag{36g}$$

Since the fourth and fifth equation pair, and the sixth and seventh equation pair are identical in (5.3), five equations with seven unknowns are obtained and naturally degree of freedom is two. Solutions of $\pi_1(w)$, $\pi_2(w)$ and $\pi_3(w)$ are unique and same with the previous case (30). There is freedom for choice of $\pi_4(w)$ and $\pi_5(w)$ depending on $c_1(w)$ and $c_2(w)$ as follows

$$c_1(w) = \frac{w_1}{\sigma} + w_2 + w_2\,w_3 - \pi_4(w) - w_2\,\gamma \tag{37a}$$
$$c_2(w) = \frac{-w_1\,w_2}{\sigma} - {w_2}^2 + w_3 - \pi_5(w). \tag{37b}$$

Thus, the regulator equations are solvable. As a result, the state feedback regulator problem is solvable for this augmented plant. Then, a state feedback control law can be formed with a 2×5 K_a matrix as described in (23). In this case, we use the previous 2×3 K matrix as the first three columns of augmented gain matrix; and set k_{15} and k_{24} to zero. By this assignment, integration of velocity error appear only quadrature-axis voltage, $\tilde{v}_q$; and similarly integration of direct-axis current error appear only direct-axis voltage, $\tilde{v}_d$. Then, the control law becomes,

$$\tilde{v}_q = k_{11}(\tilde{x}_1 - w_2) + \tilde{x}_2 + k_{14}(\xi_1 - \pi_4(w)) + w_2\,w_3 - w_2\,\gamma - \pi_4(w) \tag{38a}$$
$$\tilde{v}_d = k_{21}(\tilde{x}_1 - w_2) - w_2\,\tilde{x}_2 + k_{23}(\tilde{x}_3 - w_3) + k_{25}(\xi_2 - \pi_5(w)) + w_3. \tag{38b}$$

Now, it is reasonable to define $\pi_4(w)$ and $\pi_5(w)$ as follows:

$$\pi_4(w) = -\frac{w_2\,\gamma}{k_{14}+1} \tag{39a}$$
$$\pi_5(w) = \frac{w_3}{k_{25}+1}. \tag{39b}$$

Note that, this assignment is always possible since $\pi(0) = 0$ and $c(0) = 0$ (see (37)) as stated in Theorem 1. Hence, the control law is found as

$$\tilde{v}_q = k_{11}(\tilde{x}_1 - w_2) + \tilde{x}_2 + k_{14}\,\xi_1 + w_2\,w_3 \tag{40a}$$
$$\tilde{v}_d = k_{21}(\tilde{x}_1 - w_2) - w_2\,\tilde{x}_2 + k_{23}(\tilde{x}_3 - w_3) + k_{25}\,\xi_2. \tag{40b}$$

Then finally, the augmented control law becomes

$$\tilde{v}_{qa} = \xi_1 + k_{11}(\tilde{x}_1 - w_2) + \tilde{x}_2 + k_{14}\,\xi_1 + w_2\,w_3 \tag{41a}$$
$$\tilde{v}_{da} = \xi_2 + k_{21}(\tilde{x}_1 - w_2) - w_2\,\tilde{x}_2 + k_{23}(\tilde{x}_3 - w_3) + k_{25}\,\xi_2. \tag{41b}$$

The last step is choosing other gains in K_a matrix such that $A_a + B_a\,K_a$ is Hurwitz. In this point, it is worthy of note that the limits of uncertainty of motor parameters that do not destroy closed loop stability, can be determined according to gains of K_a matrix under the condition that $A_a + B_a\,K_a$ is Hurwitz.

6. SIMULATIONS

In this section, we have used MATLAB/Simulink to investigate the performance of the controllers proposed in the previous section. For simulations, the motor specifications are taken as in [3]: $L_d = L_q = 14.25$ mH, $R = 0.9\ \Omega$, $\varphi_r = 0.031$ Nm/A, $n_p = 1$, $J = 4.7 \times 10^{-5}$ kgm^2, and $b = 0.0162$ Ns/rad. We also have used the transformation in [3], and found system parameters as $\sigma = 5.46$ and $\gamma = -0.066$. Note that, γ is a negative valued parameter.

We have run simulations using the controllers (32) and (41). First, we have chosen a 2×3 matrix K by considering the constraints ($k_{12} = 1$, $k_{22} = -w_2$ and $k_{13} = 0$), such that $A + BK$ is Hurwitz for the controller (5.2). With the choice $K = \begin{bmatrix} -10 & 1 & 0 \\ -5 & -w_2 & -20 \end{bmatrix}$ the matrix $A + BK$ is Hurwitz with eigenvalue set $\{-21, -2.73 \pm 6.89\, i\}$.

In simulations, we have used similar scenario with [10] and set the external inputs to values, leading to chaotic behavior in open loop, such that $\tilde{v}_d = -20$, $\tilde{v}_q = 0$, $\tilde{T}_L = 5$ with initial states values of 0.01; and run simulation for 30 s. Then controller (5.2) is put into effect. From 30 to 50 s, control objective is set as $w_2 = 2$ and $w_3 = 1.5$, i.e., constant reference signals for $\tilde{\omega}$ and $\tilde{\imath}_d$ respectively. At $t = 40$ s, motor load torque, $\tilde{T}_L = w_1$, is doubled. It is followed by a set point change in reference motor velocity, w_2 to 4 at $t = 50$ s. Although not included in the controller design criteria, constant reference signal of $\tilde{\omega}$ is switched to a ramp function with 0.4 slope at $t = 60$ s. Then the reference is changed to a step of 12 and is left constant until the end of simulation time. The reference for $\tilde{\imath}_d$ current remains constant during the simulation. The results of the simulation for motor velocity and $\tilde{\imath}_d$ current are showed in Figs. 4 and 5, respectively. As seen from figures, the controller is quite effective in avoiding chaos, tolerating motor load changes and tracking set point changes. When a ramp shaped signal is preferred as reference, a small steady state error occurs. This result is acceptable since it is not included in the design criteria. Transient performance of the controller can be enhanced by tuning gains in K matrix under the constraints given before.

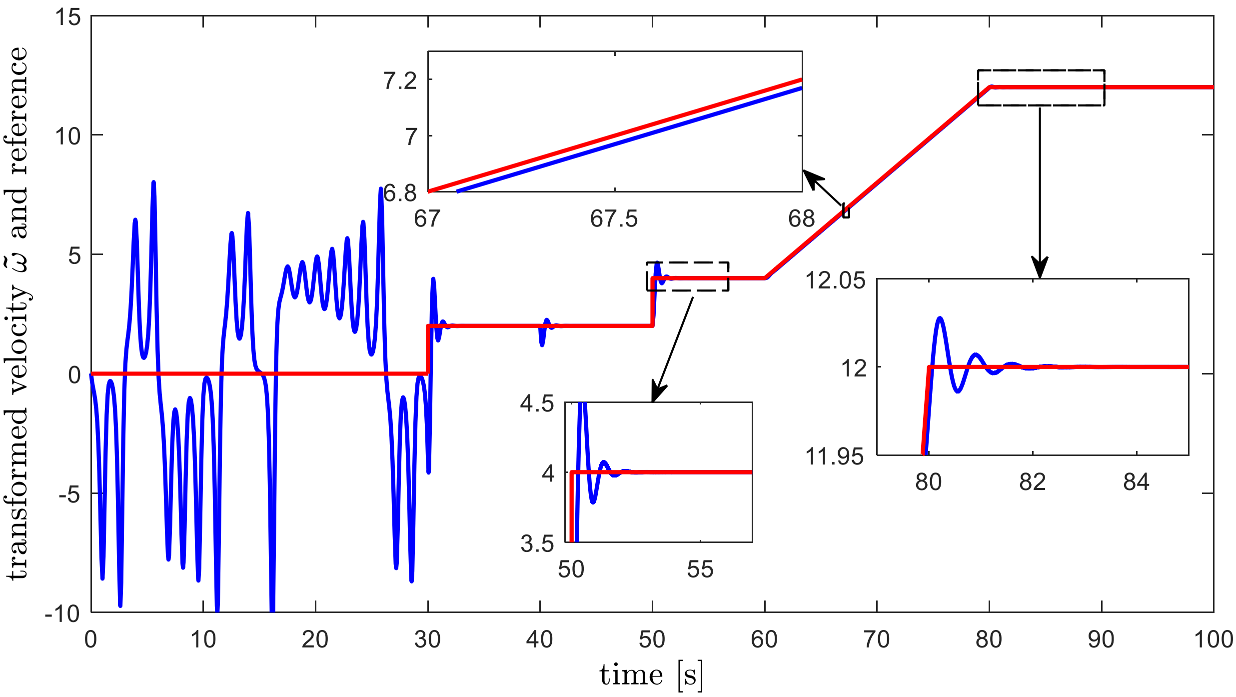

Figure 4. Simulation results for transformed velocity and its reference for first controller. Critical and indistinct points are zoomed. Actual response in blue line, reference in red line.

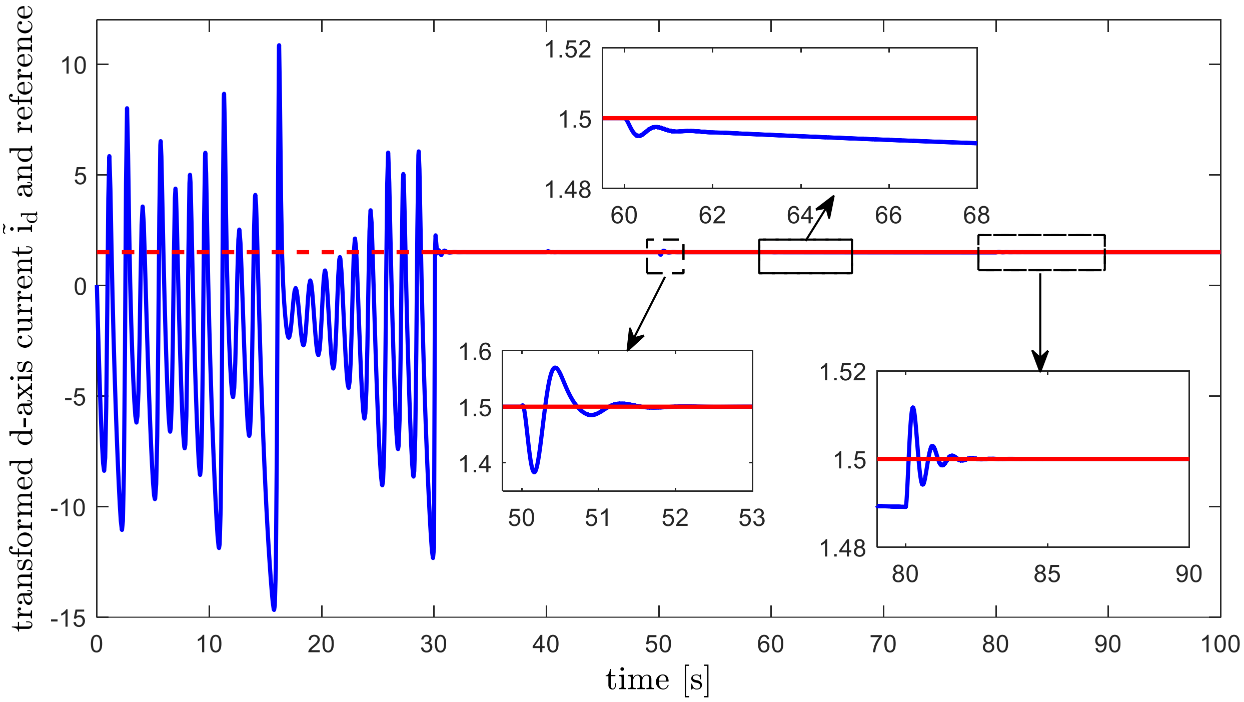

Figure 5. Simulation results for transformed direct-axis current and its reference for first controller. Critical and indistinct points are zoomed. Actual response in blue line, reference in red line.

In second simulation scenario, we have been carried out a robustness test. To investigate the robustness of the proposed controller with system parameter variation, nominal values of σ and γ parameters in the motor model are changed with a time-varying profile. Also, the measurement values of the state variables in controllers are polluted by a Gaussian noise with zero mean value and the variance of 1%.

At first system has been run in open loop, and controller has been enabled at $t = 15$. Throughout the entire simulation, control objectives are kept constant at $w_2 = 2$, $w_3 = 1.5$ and measurement noises on states are active. To investigate the effects of parameters individually, from 25 to 50 s only σ parameter and from 50 to 75 s only γ parameter are perturbed. After 75 s, both parameters are perturbed. in Figs. 6 and 7, parameter perturbations and measurement noise are shown respectively. The results of simulation are shown in Figs. 8 and 9. As seen from figures while perturbations on σ have no effect on steady state, perturbations on γ cause respectable steady state error. This is an expected result for the controller (32), since it does not involve any information about σ.

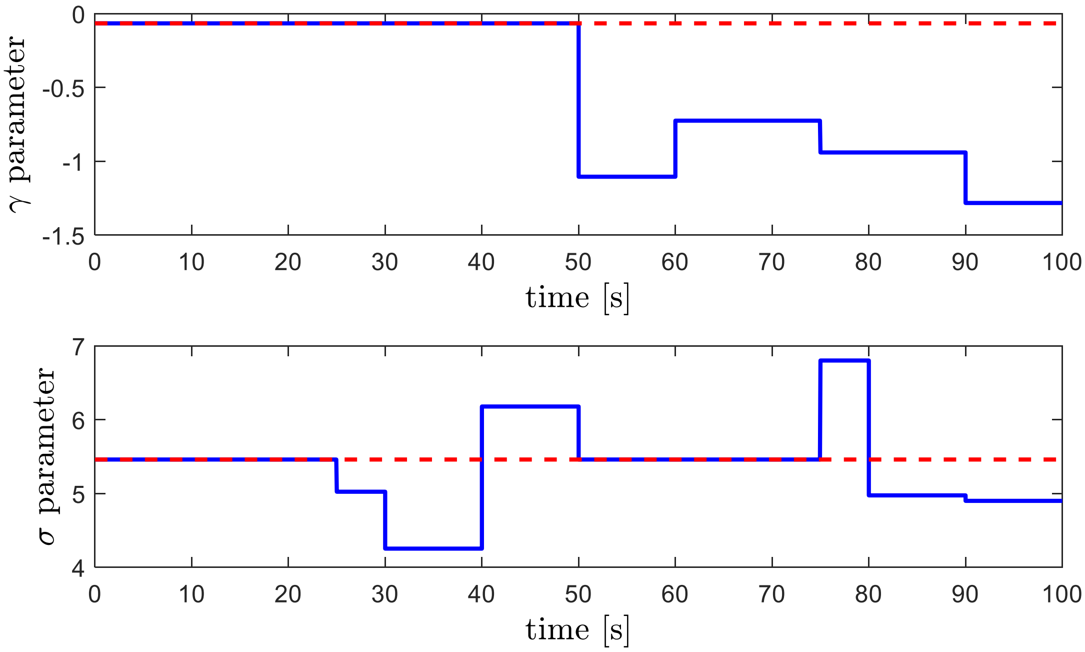

Figure 6. Variation of γ and σ parameters. Perturbed values in blue line, nominal values in red line.

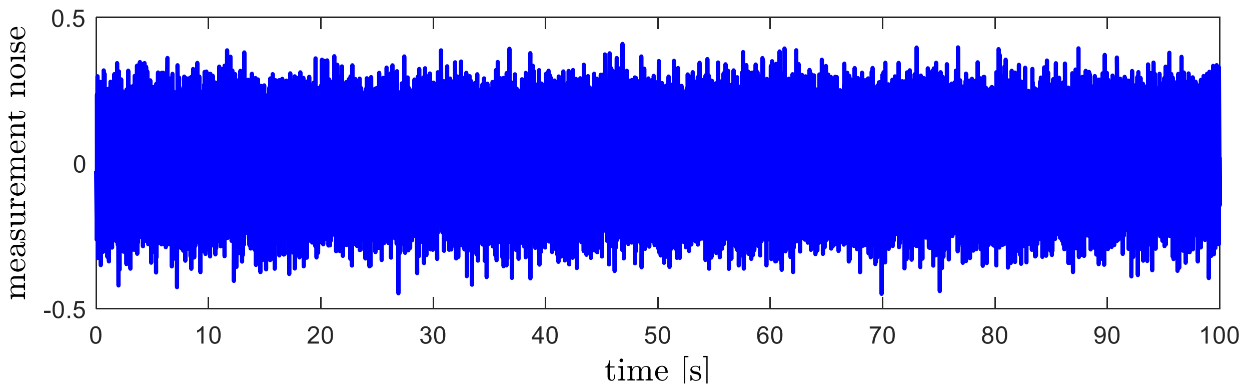

Figure 7. Measurement noise on velocity.

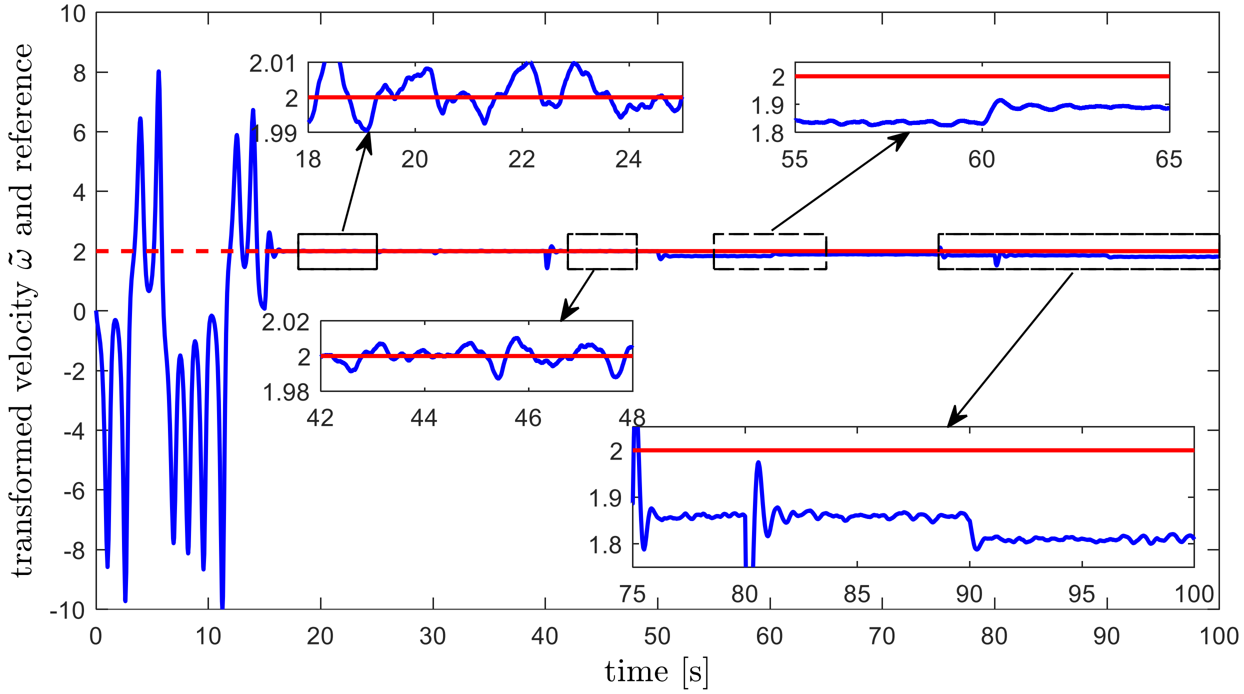

Figure 8. Simulation results for transformed velocity and its reference under parameter perturbations and noise for first controller. Critical and indistinct points are zoomed. Actual response in blue line, reference in red line.

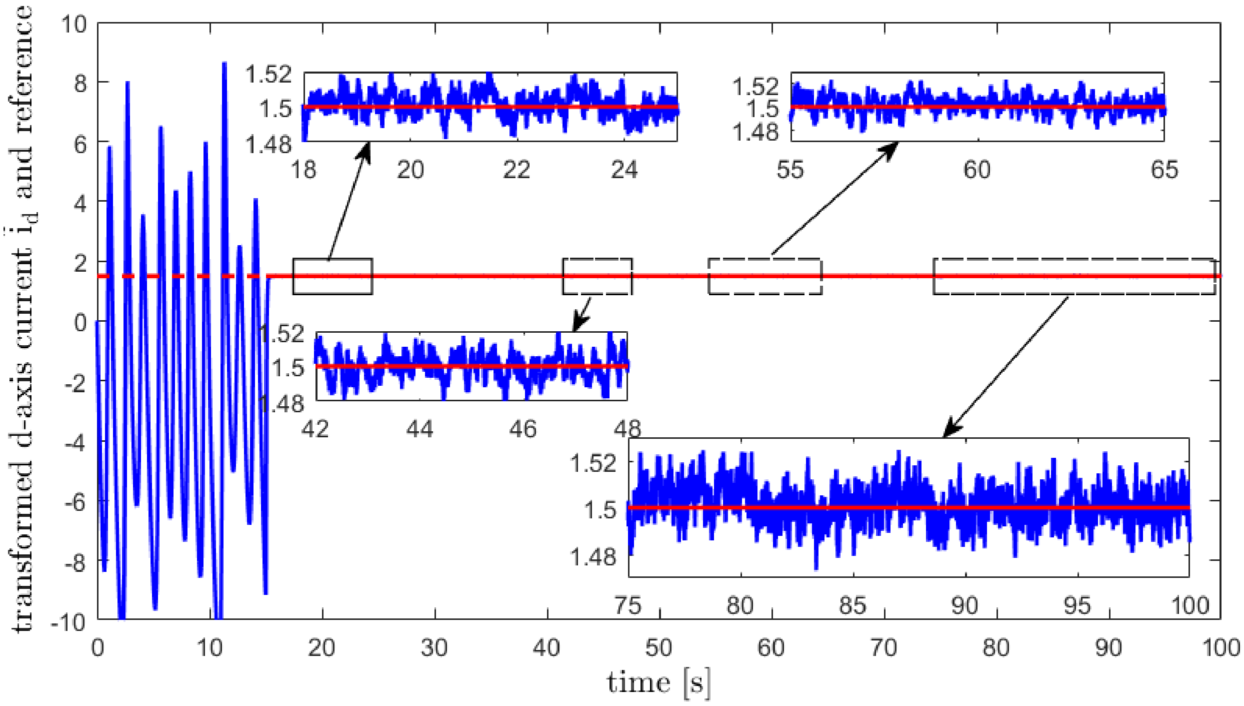

Figure 9. Simulation results for transformed direct-axis current and its reference under parameter perturbations and noise for first controller. Critical and indistinct points are zoomed. Actual response in blue line, reference in red line.

Then, we have repeated the previous two simulation scenarios for controller (41). Again at first, we have chosen the gain matrix K_a. As said before, the first two columns of gain matrix is equal to previous K matrix, and $k_{15} = 0$, $k_{24} = 0$. Other two gains (k_{14} and k_{25}) are chosen as $K_a = \begin{bmatrix} -10 & 1 & 0 & 12 & 0 \\ -5 & -w_2 & -20 & 0 & 40 \end{bmatrix}$ which makes $A_a + B_a\, K_a$ Hurwitz with the eigenvalue set $\{-18.82, -2.17, -1.44, -2 \pm 6.71\, i\}$. With this matrix choice the bounds of parameter uncertainty form as follows: If σ is less than $13/10$, then γ must be less than $\frac{-13+10\sigma}{\sigma}$. If σ is greater than $13/10$, then there is no bound for γ.

Simulations results for first scenario are given in Figs. 10 and 11 while results for scenario two are shown in Figs. 12 and 13. As seen from figures, steady state errors arising from tracking ramp function (see Fig. 10) and parameter perturbations (see Fig. 12) are eliminated since uncertainty limits are not exceeded, but overshoot increases in some cases. Naturally, transient performance of the controller can be enhanced by tuning gains in K_a matrix under predetermined constraints.

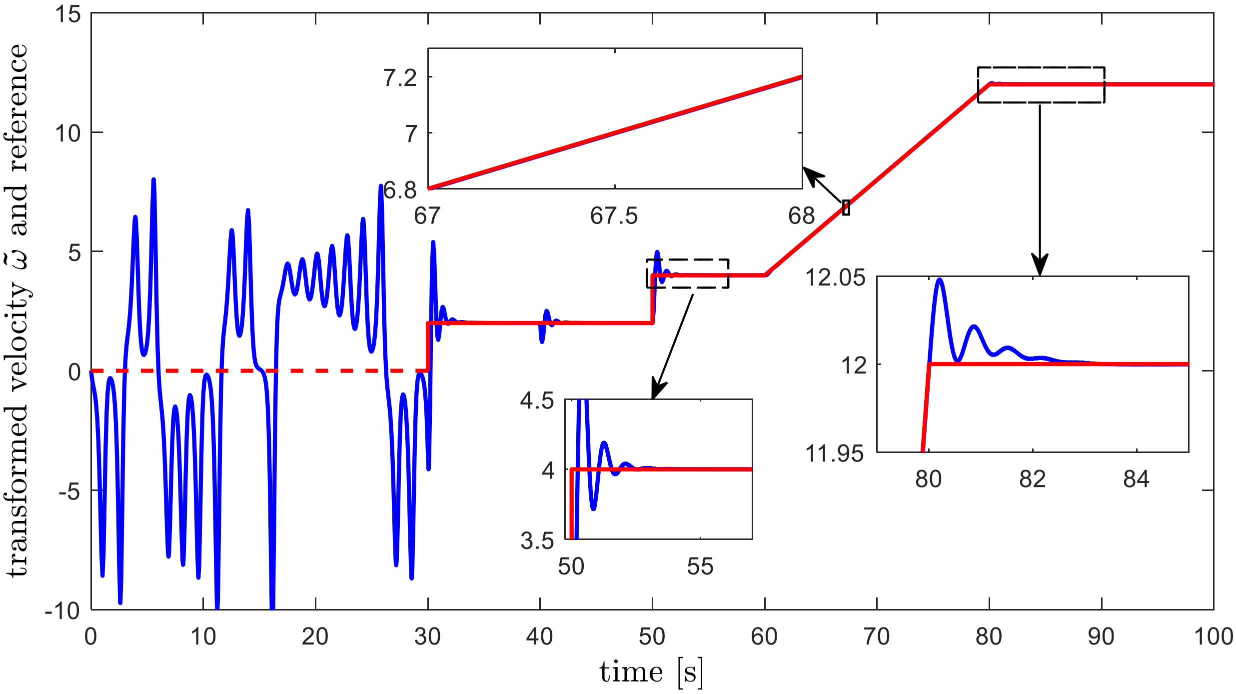

Figure 10. Simulation results for transformed velocity and its reference for second controller. Critical and indistinct points are zoomed. Actual response in blue line, reference in red line.

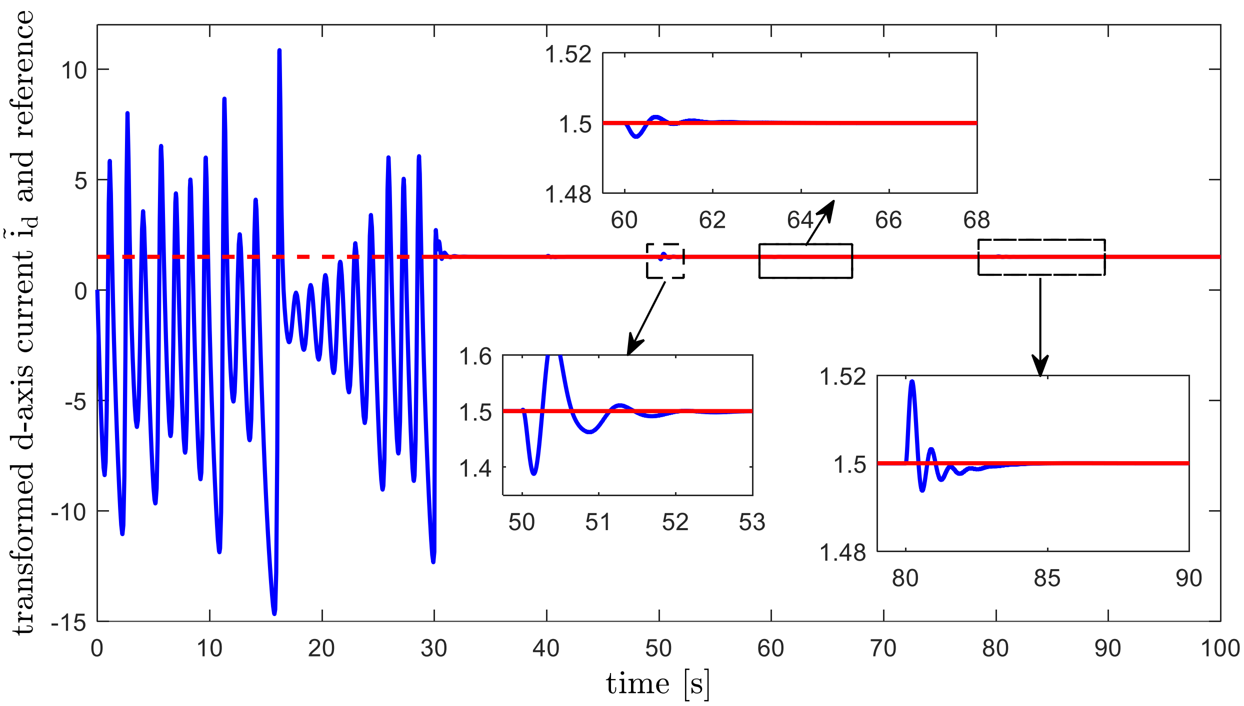

Figure 11. Simulation results for transformed direct-axis current and its reference for second controller. Critical and indistinct points are zoomed. Actual response in blue line, reference in red line.

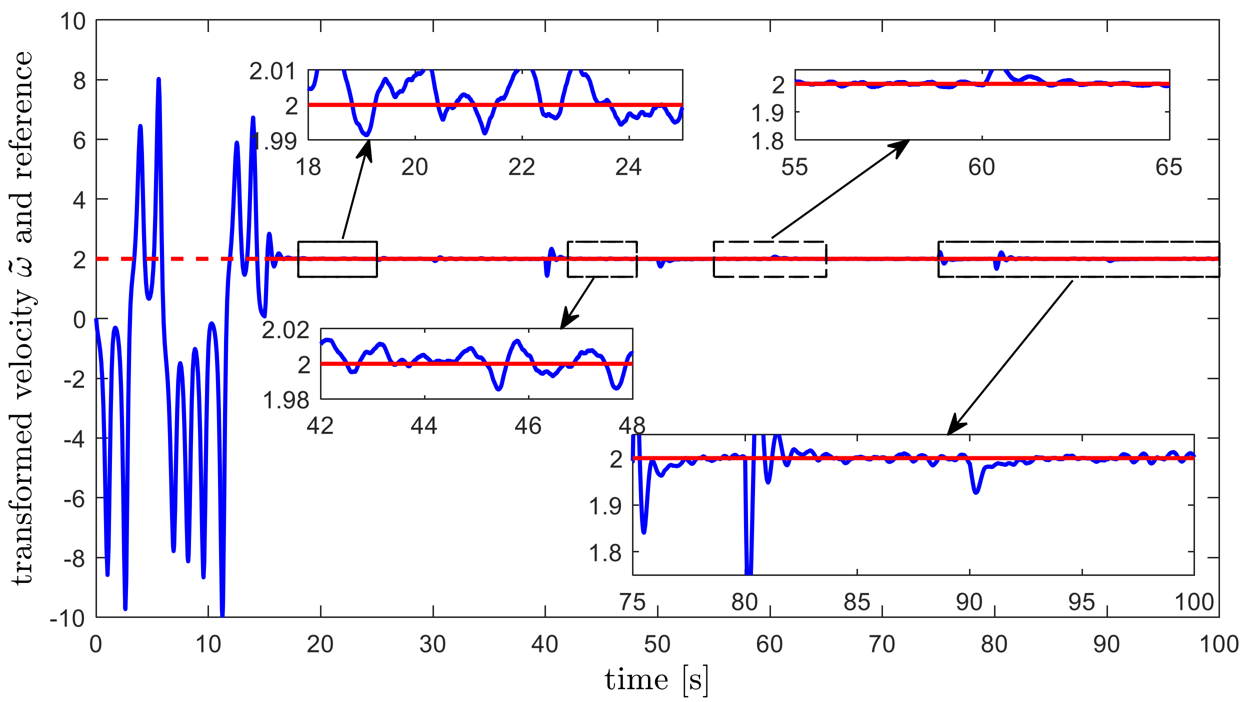

Figure 12. Simulation results for transformed velocity and its reference under parameter perturbations and noise for second controller. Critical and indistinct points are zoomed. Actual response in blue line, reference in red line.

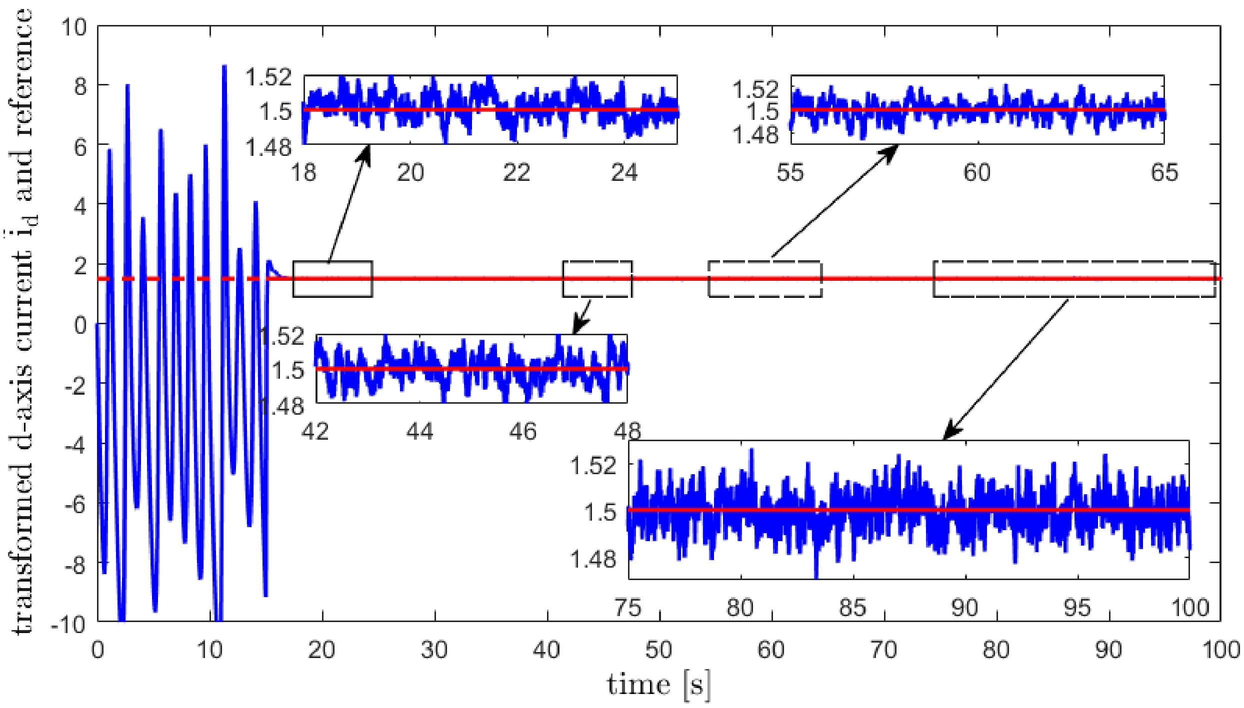

Figure 13. Simulation results for transformed direct-axis current and its reference under parameter perturbations and noise for second controller. Critical and indistinct points are zoomed. Actual response in blue line, reference in red line.

7. CONCLUSION

In this paper, first we have presented new results in chaos and bifurcation analysis of PMSM. Then, we have studied a complete solution of the output regulation problem of PMSM with state feedback control law for constant reference signals. Moreover, we have introduced integrator terms to the control law for case of parameter uncertainty. The control laws are derived using the regulator equations of C.I. Byrnes and A. Isidori in [17]. Simulation results have validated the effectiveness of proposed controllers at set point output regulation problem under parameter perturbation and measurement noise, in case of unknown load torque. Although it is out of the design criteria, the controller also exhibits quite good performance at tracking control. future work will address the experimental validation.

REFERENCES

[1] N. Hemati and H. Kwatny, “Bifurcation of equilibria and chaos in permanent-magnet machines,” Proceedings of the 32nd IEEE Conference on Decision and Control, Dec 1993, pp. 475–479 vol.1.

[2] N. Hemati, “Strange attractors in brushless dc motors,” IEEE Transactions on Circuits and Systems I: Fundamental Theory and Applications, vol. 41, no. 1, pp. 40–45, Jan 1994.

[3] Z. Li, J. B. Park, Y. H. Joo, B. Zhang, and G. Chen, “Bifurcations and chaos in a permanent-magnet synchronous motor,” IEEE Transactions on Circuits and Systems I: Fundamental Theory and Applications, vol. 49, no. 3, pp. 383–387, Mar 2002.

[4] Z. Jing, C. Yu, and G. Chen, “Complex dynamics in a permanent-magnet synchronous motor model,” Chaos, Solitons & Fractals, vol. 22, no. 4, pp. 831 – 848, 2004.

[5] Q. Dong-lian, W. Jia-jun, and Z. Guang-zhou, “Passive control of permanent magnet synchronous motor chaotic systems,” Journal of Zhejiang University SCIENCE A, vol. 6, no. 7, pp. 728–732, 2005.

[6] H. Ren and D. Liu, “Nonlinear feedback control of chaos in permanent magnet synchronous motor,” IEEE Transactions on Circuits and Systems II: Express Briefs, vol. 53, no. 1, pp. 45–50, 2006.

[7] H.-p. Ren, D. Liu, and J. Li, “Delay feedback control of chaos in permanent magnet synchronous motor,” Proceedings of the Csee, vol. 6, p. 033, 2003.

[8] D. Q. Wei, B. Zhang, D. Y. Qiu, and X. S. Luo, "Effects of current time-delayed feedback on the dynamics of a permanent-magnet synchronous motor," IEEE Transactions on Circuits and Systems II: Express Briefs, vol. 57, no. 6, pp. 456–460, June 2010.
[9] D. Q. Wei, X. S. Luo, B. H. Wang, and J. Q. Fang, "Robust adaptive dynamic surface control of chaos in permanent magnet synchronous motor," Physics Letters A, vol. 363, no. 1-2, pp. 71 – 77, 2007.
[10] A. Loria, "Robust linear control of (chaotic) permanent-magnet synchronous motors with uncertainties," IEEE Transactions on Circuits and Systems I: Regular Papers, vol. 56, no. 9, pp. 2109–2122, Sept 2009.
[11] M. Zribi, A. Oteafy, and N. Smaoui, "Controlling chaos in the permanent magnet synchronous motor," Chaos, Solitons & Fractals, vol. 41, no. 3, pp. 1266–1276, 2009.
[12] M. Ataei, A. Kiyoumarsi, and B. Ghorbani, "Control of chaos in permanent magnet synchronous motor by using optimal lyapunov exponents placement," Physics Letters A, vol. 374, no. 41, pp. 4226–4230, 2010.
[13] T. Chuansheng, L. Hongwei, and D. Yuehong, "Robust optimal control of chaos in permanent magnet synchronous motor with unknown parameters." Journal of Electrical Systems, vol. 11, no. 4, pp. 376 – 383, 2015.
[14] Z. Ping and J. Huang, "Global robust output regulation for a class of multivariable systems and its application to a motor drive system," in Proceedings of the 2011 American Control Conference, 2011, pp. 4560–4565.
[15] ——, "A control problem of pm synchronous motor by internal model design," 50th IEEE Conference on Decision and Control and European Control Conference, Dec 2011, pp. 5383–5388.
[16] W. Yu, "Passive equivalence of chaos in lorenz system," IEEE transactions on circuits and systems. 1, Fundamental theory and applications, vol. 46, no. 7, pp. 876–878, 1999.
[17] A. Isidori and C. I. Byrnes, "Output regulation of nonlinear systems," IEEE Transactions on Automatic Control, vol. 35, no. 2, pp. 131–140, 1990.
[18] J. Huang and Z. Chen, "A general framework for tackling the output regulation problem," IEEE Transactions on Automatic Control, vol. 49, no. 12, pp. 2203–2218, 2004.
[19] D. Q. Wei, L. Wan, X. S. Luo, S. Y. Zeng, and B. Zhang, "Global exponential stabilization for chaotic brushless dc motors with a single input," Nonlinear Dynamics, vol. 77, no. 1, pp. 209–212, 2014.
[20] Y. Yu, X. Guo, and Z. Mi, "Adaptive robust backstepping control of permanent magnet synchronous motor chaotic system with fully unknown parameters and external disturbances," Mathematical Problems in Engineering, vol. 2016, 2016.
[21] P. Zhou, R.-j. Bai, and J.-m. Zheng, "Stabilization of a fractional-order chaotic brushless dc motor via a single input," Nonlinear Dynamics, vol. 82, no. 1-2, pp. 519–525, 2015.
[22] P. Krause, Analysis of electric machinery, ser. McGraw-Hill series in electrical and computer engineering. McGraw-Hill, 1986.
[23] Z.-M. Ge and C.-M. Chang, "Chaos synchronization and parameters identification of single time scale brushless DC motors," Chaos, Solitons & Fractals, vol. 20, no. 4, pp. 883 – 903, 2004.
[24] C. Sparrow, The Lorenz equations: bifurcations, chaos, and strange attractors. Springer Science & Business Media, 2012, vol. 41.
[25] S. Vaidyanathan and C. Volos, Advances and Applications in Nonlinear Control Systems. Springer, 2016, vol. 635.
[26] H. Khalil, Nonlinear Systems, ser. Pearson Education. Prentice Hall, 2002.